Article:
Dijksman, J.A., Filippov, A.D., Al Harraq, A. et al. (2026) Light sheet imaging in granular materials: interdisciplinary opportunities. Granular Matter, 28 (2). 30. ISSN: 1434-5021

https://doi.org/10.1007/s10035-026-01622-2

Granular Matter (2026) 28:30
https://doi.org/10.1007/s10035-026-01622-2

REVIEW

Light sheet imaging in granular materials: interdisciplinary opportunities

Joshua A. Dijksman[1] · Alexei D. Filippov[2] · Ahmed Al Harraq[3] · Babak Vajdi Hokmabad[4] · Sujit S. Datta[4] · Elisabeth Bowman[5]

Received: 20 August 2025 / Accepted: 24 January 2026

Abstract
Granular materials, ubiquitous in geophysics, chemical engineering, biophysics and soft matter physics, present unique challenges for optical imaging due to their opaque and heterogeneous nature. This perspective paper provides a comprehensive overview of opportunities in Light Sheet Microscopy (LSM) techniques for imaging granular materials, emphasizing refractive index matching as a critical tool for visualizing internal deformations and flow dynamics. By matching the refractive indices of solid particles and surrounding fluids, researchers can create "transparent soils" or analogous systems, enabling detailed examination of particle interactions, strain fields, and fluid flow. To comprehensively introduce opportunities for future research, the review explores the evolution of LSM, from early broadband light sources to modern laser and LED-based systems, highlighting advancements in wavefront shaping and contrast generation through scattering and fluorescence. The paper also surveys some innovative approaches for LSM and index matching, such as Sephadex spheres and cryolite. Emerging techniques, such as wavefront shaping and three dimensional imaging with event cameras, are presented as promising avenues for future research. Additionally, the review connects granular imaging to biological systems, demonstrating its relevance for studying microbial motility, biofilm growth, and tissue engineering. This perspective paper aims to guide and inspire researchers in selecting and refining LSM techniques for advancing the understanding of complex particulate systems.

Keywords Granular materials · Grains · Hydrogel spheres · Clay · Light sheet microscopy · Index matching

1 Introduction

As eloquently captured in the opening statement of a classic materials science book by [1], materials are neither point particles nor rigid bodies; materials *deform*. Whereas the motion of point particles and rigid bodies is easily measured, visualizing the flow and deformation of the interior of a material or a structure presents profound experimental challenges for science and engineering. Many solutions for these challenges have been put forward in recent decades, each suitable for a particular range of applications and settings. Here we focus on the imaging of powders and particles, or "granular materials". Their deformation and flow measurement is most often and easily done using visible light, due to the abundance of optical components, cameras and light sources available, especially since the dawn of mass consumer market digital photography. To use such visible light to image the interior of a granular material requires the use of transparent materials, and in a granular

Ahmed Al Harraq and Babak Vajdi Hokmabad contributed equally to this work.

✉ Joshua A. Dijksman
j.a.dijksman@uva.nl

✉ Elisabeth Bowman
e.bowman@sheffield.ac.uk

1 Van der Waals-Zeeman Institute, Institute of Physics, University of Amsterdam, Amsterdam, The Netherlands

2 CNRS, Institut Charles Sadron, Université de Strasbourg, 67200 Strasbourg, France

3 Joseph Henry Laboratory of Physics and Lewis-Sigler Institute for Integrative Genomics, Princeton University, Princeton, NJ, USA

4 Division of Chemistry and Chemical Engineering, California Institute of Technology, Pasadena, CA, USA

5 School of Mechanical, Aerospace and Civil Engineering, University of Sheffield, Sheffield, UK

Published online: 11 February 2026

context, this implies the use of "refractive index matching". In refractive index matching, the solid particle phase is made of transparent material, which is then immersed in a transparent fluid with the same refractive index. The resultant transparent mass, or "transparent soil" is so made accessible for imaging. Such imaging can provide information about the sought-after deformation field at a point, in a plane or over an entire volume, depending on the imaging method used and aims of the research.

As we shall see, developing index matching experiments can require considerable resources. To obtain deformation or strain fields, numerical methods are typically much less involved, such as Finite Element modeling or Discrete Element Methods. In our view, index matching methods are still necessary: first of all, experimental investigations can calibrate or validate numerical approaches that try to locally describe the deformation of a material. More importantly, experimental approaches also *inspire* new numerical approaches, as the latter always contain (coarse-graining) assumptions that are either too restrictive or not applicable at the relevant time and lengthscales of the system under study. For example, the physics of particle-particle interactions in a suspension involves both frictional and viscous forces, the balance of which decides the fate of the material [2]. While numerical simulations have certainly guided developments in the field, experimental, microscopic insights in these complex processes are still needed. The same is true for numerically challenging multiscale problems such as soil physics, in which particles ranging in size from submicron to centimeter can determine its deformation behavior [3]. Additionally, computing the interactions between *deformable* particles is still a formidable numerical challenges, in which experiments can provide a guiding light to efficient and accurate algorithms [4]. Refractive index matching can even aid in internal stress imaging via two and three-dimensional photoelastic methods [5–7], further supporting developments on constitutive modeling.

There is a growing number of internal imaging methods, and a growing number of materials known to be suitable for refractive index matching. The aim of the current Perspective is twofold. First of all, we aim to inform the reader interested in "granular materials" of some (for them) potentially interesting yet (to them) unknown methods used in index matching methods across time and disciplines. We connect index matching specialists and enable them in one comprehensive document to learn about existing methods from different fields that could work for them. We do so by highlighting the long arc of history of the refractive indexing and slight sheet imaging methods and citing some relevant yet under-cited works from the past. We cover several structure/flow imaging methods that are used in the different disciplines that touch upon granular materials, such as geophysics, geomechanics, chemical engineering, biophysics and soft matter physics. We place these methods in context of existing literature reviews from the aforementioned fields but also linking them to method developed in other fields, such as biology, that also involve optical imaging methods. Some approaches mentioned in the different corners of the literature partially or completely overlap in their methodology and nomenclature, which we clarify along the way.

Second, we aim to indicate some promising *future* avenues of research. We do so by updating the reader on some lesser known methods, techniques and materials that can be useful to *simplify* their specific application, given the known limitations of state of the art methods, including safety concerns with some materials. We also provide some imaging method examples that have not yet been extensively used in the granular materials fields, yet do provide ample opportunities to explore new research directions. In this context, we provide guidance on how to perform microscopy and index matching on *soft* and *biocompatible* samples.

We focus on light *sheet* illumination, and while we cover a broad range of methods and potential applications, we have a particular emphasis on methods used for flows in which the particles do not just act as tracers, but in which they affect or compose the entire flowing material. We take this challenge because the inclusion of distinguishable particles sets some of the strictest limits on the optical methodologies employed and discussed here. To achieve the index matching requirements necessary for some of the methods, we also review new and classic literature on materials and, in particular, Christiansen cells [8], which can be employed to systematically test and tune index matching materials [9].

Materials imaging based on visible light and its "sheet" variants are generally known as Light sheet microscopy (LSM) [13]. LSM is known across a range of fields as: Ultramicroscopy (UM) [14]; Orthogonal plane fluorescence sectioning (OPFOS) [15]; Selective Plane Illumination (Fluorescence) Microscopy (SPIM) [16]; Planar Laser Induced Fluorescence (PLIF) [17–19] and, Refractive Index Matched Scanning (RIMS) [20, 21]. LSM stands in contrast to the intrinsically one-dimensional methods such as Laser Doppler Anemometry (LDA) or Optical Coherence Tomography (OCT). The dynamics or flow imaging variant of LSM is usually tracer-based and complemented with image analysis techniques such as Digital Image Correlation, also known as Particle Image Velocimetry (PIV), and the separate technique of Particle Tracking Velocimetry (PTV) methods. X-ray based tomographic methods can also be considered intrinsically three dimensional, as such tomography is based on the material's absorption characteristics and can hence only be done in 3D reconstruction [22].

To place developments and use of LSM in a broader context, it is useful to consider one-dimensional methods when considering flow measurement techniques for a given scientific question. These one dimensional methods are generally based on light interferometry and came on the scene after the invention of the laser in the 1960 s, as they rely on coherent light sources. They often have the benefit of giving very high imaging rates and additional flow information [23]. Two-dimensional methods are always light sheet based and also have a long history because light sheets are easy to make. Two dimensional methods can be extended to three dimensions by imaging multiple sheets sequentially. There is also intrinsically three dimensional imaging, by which we mean here the methods based on flow heterogeneity or tracer particle tracking via the simultaneous imaging of a flow with several aligned cameras (tPIV, tPTV). An overview of the intersections of the various methods used for flow imaging is provided in Fig. 1. In this figure we trisect light sheet flow imaging methods based on the light source that can be used for it: broadband wavelength, single wavelength or both. To further enhance the overview of the methods, we show various methods of producing contrast or imaging structure to a light-sheet based imaging method. As points of reference, we indicate some key historical references, among which the first light sheet microscopy reference from [10], the first index matching of solids and liquids in so-called Christiansen filters [8], and the earliest reference known to us on index matching, laser-based study of deformations in dense particle packings [11]. We also indicate in Fig. 1 the new opportunities for a combination of laser + fluorescence based imaging of microstructure, especially when combined with structured laser beams and

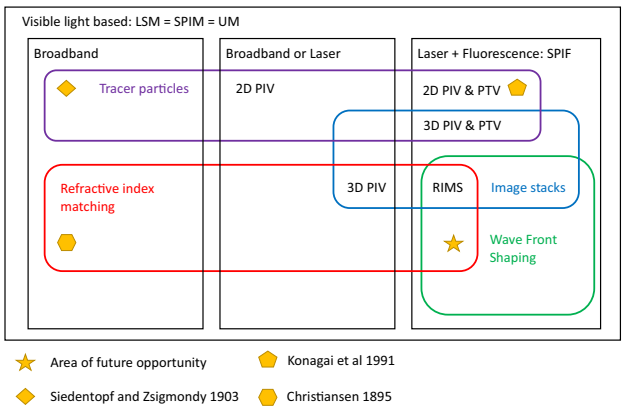

Fig. 1 A schematic overview of visible light based light sheet microscopy methods. The three rectangular areas indicate microscopy using either broadband light, broadband or laser or just laser and perhaps fluorescence. Within these domains, contrast methods based on tracer particles (purple box), fluorescence (blue), direct scatter (red) or wave front shaping (green) are indicated. The methodologies of classic works from Siedentopf and Zsigmondy [10], Konagai [11] and Christiansen [12] are indicated, as well as an area of future opportunity ($\star$)

index matching via nowadays commercially available light sheet microscopes—see Sect. 2.2.

We structure the paper as follows. In Sect. 2, we first cover the various "light sheet" technology options to clarify how light sheets can be combined with various different contrast generating methods, to be able to highlight recent advances. We then delve into then digital image recording methods in Sect. 3 and image analysis methods that are typically employed to extract deformation fields. We explore opportunities for new material choices for LSM and index matching in Sect. 4, and introduce a number of current and future applications of refractive index matching methods in Sect. 5.

2 Lights sheets, optical phenomena & contrast

The light sheet is evidently a core component of any light sheet microscopy application. A sheet of visible light can be made in a surprisingly large number of ways, greatly enhancing the application of light sheet imaging across a number of fields. Here we cover the basic considerations of light sheet physics for imaging different types of materials. We organize this section by the properties of the light sheet: its wavelength domain, and, for coherent monochromatic light, the phase modulation method. The latter is a recent development in biophysical imaging that makes it possible to perform light sheet imaging in even weakly index matched (biological) samples, which we consider to be of relevance also for materials science applications [24].

2.1 Broadband light sources

The first light sheet tomography was performed in the early 20th century by Siedentopf and Zsigmondy [25]. Their light sheet was based on a broadband light source, namely the Sun. The effective use of broadband light shows that light sheet microscopy is a broadly useful method that for its basic principles of operation does not require sophisticated light sources or optics. Generally speaking, broadband light sources can reach very high intensities, favoring them for large scale and/or very high speed imaging conditions. However, there are two main drawbacks to using a broadband light source. First, the broadband light will suffer from dispersion inside the medium: the light sheet geometry will be affected by variation of the index of refraction $n(\lambda)$ with the range of wavelengths λ coming from the light source. Second, with a broadband light source, contrast can be generated only by absorbance or direct (Rayleigh) scattering of the light from impurities. Fluorescence-based imaging is not possible in broadband mode, since the emitted wavelength

will overlap the spectrum of the light source. Furthermore, fluorophores lose their fluorescence due to photon-induced degradation ("bleaching") at the high intensities characteristic of broadband sources. These two considerations were not restrictive for the low-density gold nanoparticle suspension that Zsigmondy was studying. However, modern applications of light sheet microscopy usually involve complex samples with more internal microstructure and chemical contrast agents. The use of broadband light sheet sources has therefore declined in favor of single-wavelength or monochromatic light source sheets.

2.2 Single wavelength light sources

Single wavelength light sources have been available since the emergence of gas luminescence (sodium and mercury lamps in particular) and coherent single wavelengths have been around since the invention of lasers. In the last two decades, the range of single wavelength sources has been expanded by the use of (cheaper) light emitting diodes (LEDs). The benefits of single wavelength light sources directly compensate the drawbacks of broadband sources. For example, the use of single wavelength sources reduces dispersion effects and increases contrast options to include fluorescence. With lasers, coherence length options become an additional benefit of monochromatic light sources, and wave front modulation is nowadays a regular tool to remove scattering effects for samples with internal refractive index variability. A benefit of laser and LED based illumination is that they typically have a short response time, allowing their light to be precisely timed with image recording to limit heat generation, bleaching or other detrimental effects. Even so, monochromatic light sources are still mostly of lower intensity, and their use has been relatively expensive compared to broadband light sources until very recently.

Lasers—Lasers have been used for flow imaging for many decades, as a simple literature search can reveal. In recent years, diode lasers have become very affordable to the point that a low budget can already provide the necessary power for many applications. Laser output stability can also be better controlled, resulting in more time-independent lighting conditions in experiments, which helps subsequent data analysis. Diode lasers can also be easily turned off when a respective sample is not being imaged, which helps against the photon-induced degradation of fluorescent dyes, as described in e.g. [19, 21]. Commercially integrated systems that can image milliliters of sample volume are readily available, such as the Zeiss Lightsheet microscope; traditionally used for biophysical research on single organisms, it can also be used for particle imaging, as in Fig. 2, where we show sample images of labeled Sephadex spheres (see Sect. 4.1) and poly(methyl methacrylate) (PMMA, acrylic) spheres (CA20, microbeads.com). We will turn to other sheet imaging materials and methods useful for biophysical purpose in Sect. 5.3.

LED—Light Emitting Diodes (LEDs) offer a low cost alternative to lasers as a monochromatic light source [26] and they can be used to measure fluid flow via PIV [27]. Despite this, only limited studies have been published that use LEDs with refractively matched granular systems – for example [28] who used LED sheets to illuminate fluid flow around hydrogel beads. Hence it would appear that the

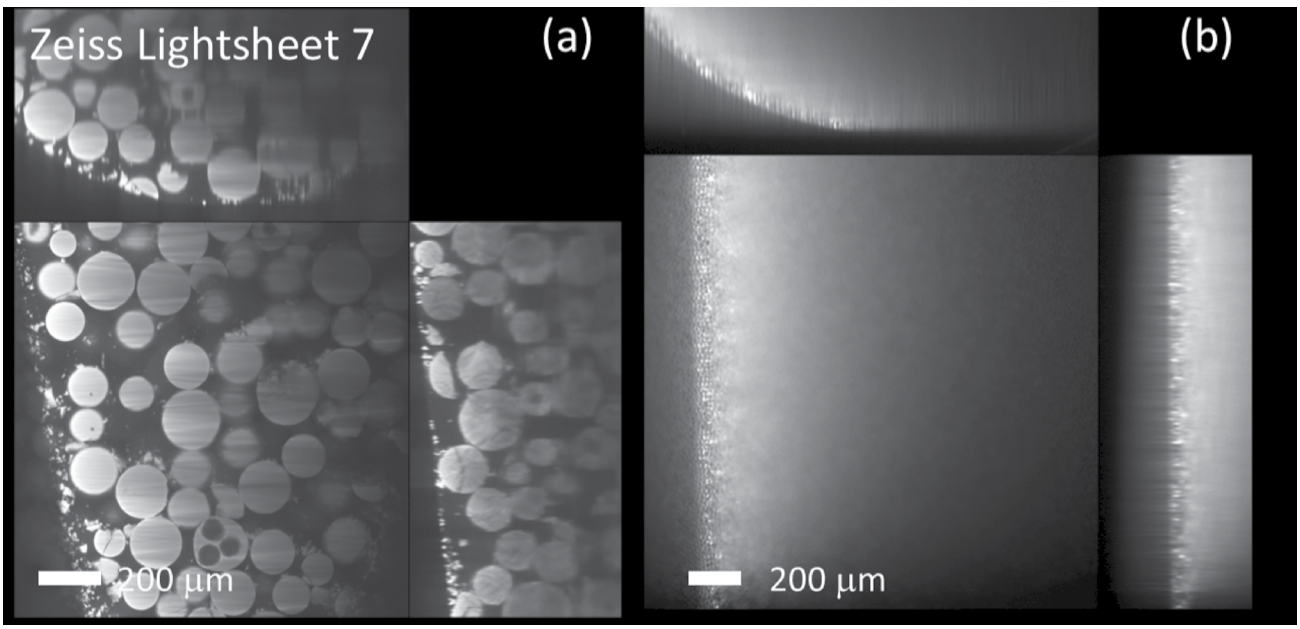

Fig. 2 Commercial light sheet 3D microscopy examples provided courtesy by Zeiss, from their Lightsheet 7. **a** labeled Sephadex spheres **b** 20 micron acrylic spheres (Spheromers CA20, microbeads.com) in water

visualization and measurement of granular behavior using this technique has yet to be fully realized.

2.3 Light sheet optics

The optics behind light sheet microscopy have been described in detail in several reviews, e.g. [13, 29], including detailed explanations of how to build such instruments. The most trivial way to generate a light sheet is to create a Guassian-like beam from a polychromatic source, or use a Gaussian beam from a laser, to stretch one of the axes of the profile using a cylindrical lens. While this is relatively simple, it also comes with the drawback that the illumination intensity along the line is not uniform and strongly dependent on the distance from the laser source; see e.g. the USB driven "PL" laser series from Thorlabs [30], which then requires extensive calibration of the method and/or post-processing of the image data. To reduce these experimental and analysis complexities, optical components have been developed that generate a uniform intensity line – e.g. Powell lenses. The drawback of such optics is that they reduce the transmitted output power of the beam, but the intensity reduction is usually less than 50%. Non-trivial ways to extract more penetrative ability from the light sheet is via *wave front shaping*.

Optics can reduce the need for index matching—The passive form of wavefront shaping is used primarily in the biomedical field [31] and is already available in commercial microscopy applications. As examples, we show images of soft and more rigid spherical particles imaged in the Zeiss Lattice Lightsheet 7 microscope in Fig. 4. Both the Sephadex and acrylic spheres can be imaged with high resolution, despite the complete lack of index matching between the solvent and the particles. The method relies on light sheet patterning with optical elements that both reduces photobleaching and offers higher resolution. Another such method that can be used for imaging is active wavefront shaping [32].

Active wave front shaping can be used to image highly turbid media, but requires feedback control over the optical element that controls the light sheet. Its use for flow measurements so far has been limited, but it can be achieved as shown in [33].

2.4 Generating contrast

To image a flow or deformation field it is necessary to be able to *identify* similar patches of the material of interest in subsequent images. The necessity of imaging patches of a material consistently, frame to frame, means one has to get light from the source selectively into the camera. This "Lagrangian" approach to measure flow or deformation can then be used later to e.g. obtain a (time-averaged) Eulerian perspective of the deformation field. To identify patches in subsequent images, all kinds of contrast methods can be used. Contrast elements need not be discrete (tracer) particles, but these are the most commonly used objects to allow for material deformation analysis. In general, any material property that varies in space and is reasonably coherent or *steady* between time points can be used to image deformations: refractive index, absorption, turbidity, color, and density fields can all be used if the respective field can indeed be measured (indirectly). If a fluorescent label is sensitive to physical variables such as pH, viscosity or temperature, such fields can also be imaged [19].

Light sheet microscopy usually relies on either of two contrast-generating methods: scattering and fluorescence. When the sheet illuminates the material, either the light sheet directly scatters its photons off a tracer element in the direction of an imaging device - the displacement of tracers then allows for deformation analysis; alternatively, the material locally absorbs the light from the sheet, to have it fluoresce a dye that is locally embedded in the material. The variability in dye concentration then provides the contrast. These two methods of creating contrast have different benefits and drawbacks which we discuss in the respective subsections.

Scattering When a photon traverses a refractive index boundary, it has two options: refraction or reflection. The detected light intensity is the collective result of numerous boundary-traversing events at a given position from the sample origin. The seeding of fluids using neutrally buoyant ($St \ll 1$) tracer particles enables the tracking of fluid flow, independent of the position of particles within the flow. In the case of media where the grains and fluid are considered to be a single phase, e.g. in a geomechanics context with the very short-term shearing behavior of saturated sands and short-to-medium term deformation of clays, the use of seeds or tracers that reflect light within the laser plane can allow the bulk deformation of the material to be viewed and quantified using image analysis methods such as PIV; see [34] and [35].

We note that laser speckle describes the phenomenon where the coherent light from a laser interacts with the granular medium under investigation. In case the light scatters multiple times within the medium, the result is a scattering of light seen as "speckles" within the laser plane. This speckle itself may be sufficient to produce the required image "texture" for analysis [36] and to extract quantitative information about local deformation [37, 38], although it is more common practice to add tracers. In the situation where laser speckle is unwelcome, it is relatively straightforward to filter out.

Fluorescence Scattering has the intrinsic trade-off that increased contrast comes at the price of decreased optical depth. When emitted by probes that are index-matched to their environment, fluorescence allows for contrast without compromising transparency. The invention of lasers made fluorescence-based imaging possible due to the attendant use of laser dyes and color filters. Laser dyes can bleach over time under the influence of light, which limits the amount of light one can use to make the laser dye fluoresce. The relevant factors to consider for fluorescent imaging are manifold, and depending on the application, these properties are either a hindrance or an desired feature. We list some below; more can be found elsewhere [19, 21].

- Lifetime: there are short and long lived fluorescent dyes that radiate their emitted photons within a picosecond up to milliseconds after being illuminated. The fluorescence or phosphorescence delay can be useful or detrimental to the imaging of the flow.
- The Stokes shift is the difference between the absorbed and emitted photon, and needs to be large enough to separate them, but must also be small enough to not suffer from dispersion, as index matching depends on the wavelength.
- Fluorescent dyes are notoriously sensitive to their chemical and physical environment, such as pH [39] and sometimes local stress (mechanofluorescence).
- The quantum efficiency of a dye indicates how efficient the dye is in converting captured photons to emitted photons. The higher the quantum efficiency, the less dye one needs.

Using fluorescence-based LSM then requires a tuning of the light sheet and dye to the application, relevant materials and scientific question.

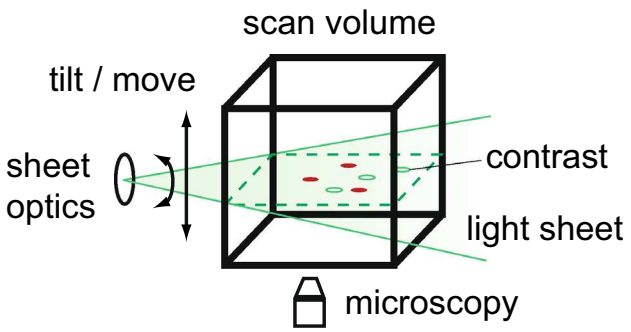

Fig. 3 The main components of any LSM: a light sheet, a microscopy setup or camera configuration and a method to move the imaging plane through the sample. Contrast agents can be fluorescent (red dots) or scattering agents (green circles). The sample volume can range from mm^3 to m^3

3 Imaging & analysis in 2D and 3D

3.1 2D: planar light sheet imaging

To reconstruct a deformation field in a material in three dimensions, a three dimensional image of the material must somehow be reconstructed. A straightforward method to do so is by imaging a 3D volume slice by slice, creating an image stack. Laser sheet imaging does just that, as has been developed over the last decades in different fields [19, 21]. The basic principle is always the same: a sheet illumination is created with a laser and the appropriate optics for the dimensions of the object of interest. The sheet illuminates the sample and the reflected, refracted or fluorescent light that generates the contrast in the plane is captured by a camera via a microscopy setup or lenses to image a sheet. After obtaining one image, the sheet is moved a small amount inside the sample, either by moving the sample, or the sheet via translation or rotation. A sketch of the working principle is shown in Fig. 3. One of the main benefits of light sheet imaging with respect to single point (confocal) imaging of a sample, is that scanning an additional dimension is much faster, reducing both overall experiment time and dye bleaching. To image a three dimensional system, one moves the sheet through the sample either by moving the sample or the sheet— see Fig. 3. In most smaller systems, optical components remain static while imaging and the sample is translated or rotated. When sample motion becomes challenging due to its inertia or integration in other components (e.g. microfluidics) it is also possible to sweep the sheet with optical means. The light sweep design process has multiple considerations: rotation can enhance resolution; sweeping can enhance the field of view. There are open source manuals available on building a RIMS setup [40]. An open platform has the benefit of low cost and flexibility in terms of size and application area. For those with deeper pockets, microscopy companies such as Zeiss and Nikon also offer commercial solutions for index matched laser sheet based imaging of small samples.

Event cameras The sheet motion needs to be optimized for a given material of interest, a microscopic observable of interest, contrast agent, camera speed, et cetera. We focus here on both static and dynamic imaging of dense granular media. The choice of camera is evidently important; there is a incredible range of high speed and high sensitivity, hyperspectral and polarized light cameras available nowadays. No review of that would do justice to that here. We would like to highlight the emergence of "event cameras" that do not track the total light collected per spatially extended region, but rather the (thresholded, binarized) *change* in light intensity. The operation of event cameras mimics the functioning

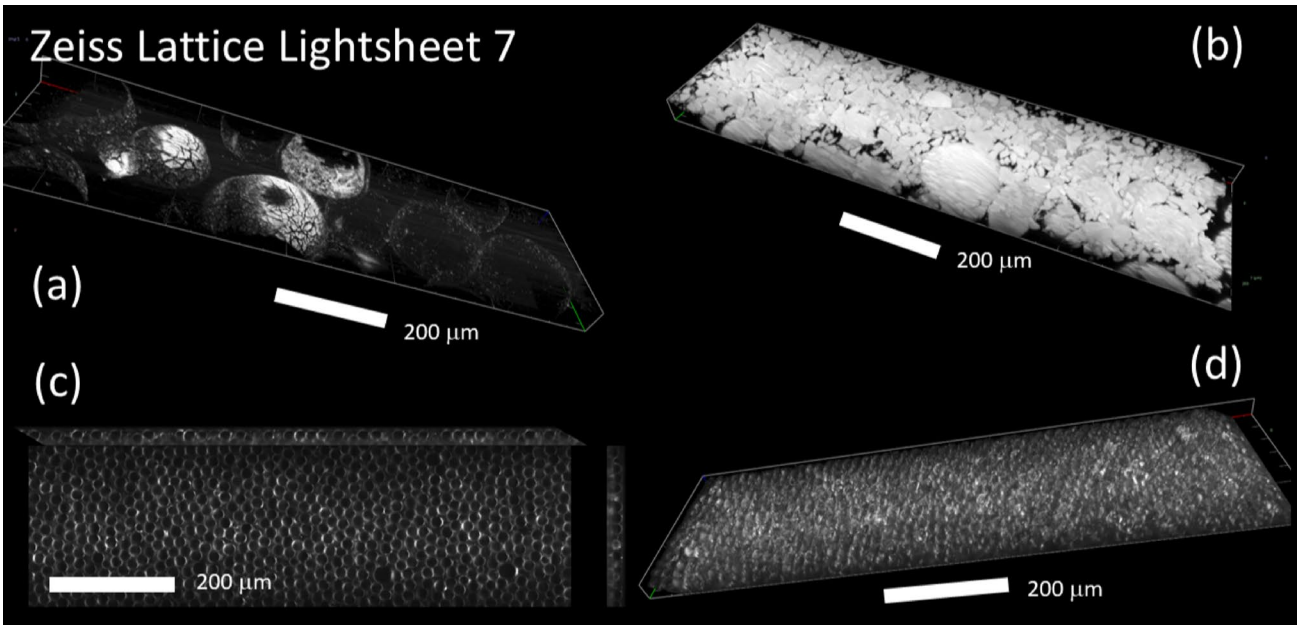

Fig. 4 Wave front shaping 3D microscopy examples provided courtesy by Zeiss, Lattice Lightsheet 7. **a**, **b** unlabeled Sephadex spheres (**a**) and fluorescently labeled fragments (**b**). **c**, **d** 20 micron acrylic spheres (Spheromers CA20, microbeads.com) in water

of the retina [41–43]. Event based imaging has the benefit of allowing for vastly higher frame rates, but comes with increased complexity in extracting physically relevant parameters from the data. An example camera is the Lucid Triton HDR camera range.

3.2 3D imaging—steady state

Under steady laminar fluid flow it is possible to create an image stack by successively imaging the medium at increasing depth. If the images are stacked closely enough compared to the minimum particle size, post processing can enable a 3D reconstruction of the grains, pore morphology and, if tracers are included, fluid flow velocity to be carried out. An example of this is [44], where machine learning was used to facilitate a 3D construction of the fluid flow around approximately 20 densely packed particles, which was then compared to a numerical model of the fluid-particle system to obtain local particle forces. Both spherical and angular particle packings were examined.

An alternative to imaging from a single direction is to take orthogonal viewpoints and create two or more sets of image stacks. Linear interpolation can then be used to construct the grain and pore morphology along with steady fluid flow, if tracers are included. This method was used in [45] to obtain high-fidelity fluid velocity measurements using a PTV-type approach.

3.3 3D: tracer particles in transparent media

Broadband light (such as from the Sun or a standard lamp) can also be used to examine internal microstructure of a granular-fluid system. In such an arrangement, two orthogonally placed cameras with large depth of field are needed to image over the depth of interest and then to establish the 3D relationship between tracer images using a statistical approach, in order to determine the 3D coordinates of specific tracers through time. PTV may then be used to describe the fluid velocities, as in other studies. An example is [46] and subsequent work, where vertically ascending air bubbles were used as tracers within a refractively matched system under upward flow.

3.4 3D: refractive index matched scanning

LSM and its variants are limiting in the case where the light sheet encounters many interfaces of refractive index mismatch. Even the slightest variation of refractive index, of the order of 10^{-3}, can create artifacts such as stripes due the lensing in the plane of the sheet. Also sheet disintegration due to out-of-plane sheet scatter can occur, making the light intensity gradients in the sheet stronger, and potentially dependent on particle flow itself.

Each of these issues, as well as inevitable impurities within the material will result in the decay of optical clarity with depth into the medium, due to light scattering off points of mismatch. Individual arrangements need to be assessed and modified to maximize clarity. In situations

where the presence of tracers in front of the plane of interest may obscure the image plane sought, it may be possible to limit tracer placement to the particular region of interest well within the experiment [35].

One solution that avoids such sheet integrity issues is wavefront tuning, as is done in LSM with Bessel beams. Another solution is to adjust the refractive index of the materials in such a way that there is no refractive index mismatch (or one can combine both). To achieve refractive index matching, there are a few experimental considerations to be taken into account.

Recently, light sheet imaging for biological samples has reached a point that many review articles on the subject have appeared [47–49]; it has even been called "The light sheet microscopy revolution" [13]; several commercial solutions for Refractive Index Matched Scanning (RIMS) are already available and even used for complex fluids [24].

3.5 Strain field imaging: PIV & PTV

For the physical modeling of many granular material systems, such as geotechnical systems, geophysical hazards and powder processing, it is common to track particle deformation fields, and hence strain fields, at the sidewalls of plane strain experiments under load. As an extension to this, where problems are not planar but rather, deformations occur in three dimensions, refractively matched granular media may be used [50], along with appropriate techniques to track deformations within the interior of the medium. Here we discuss techniques that may be used for specific problems.

First, when the deformation field within a medium is of interest, the plane in question must be defined by illumination. This is usually done using a planar light sheet that may be moved successively and / or orthogonally to build up a three dimensional tomographic picture (if required) in steady state or steady flow situations. The next consideration is to obtain images that are of sufficient quality, which may involve pre-processing to improve contrast and reduce noise and light inhomogeneity. Subsequently, displacement or velocity tracking may be applied [51] as discussed hereafter.

3.6 Postprocessing images

Particle Image Velocimetry (PIV) can be used to trace fluid flow within a granular medium or the movement of collections of grains / particles themselves. The application of PIV involves first discretizing images into specific interrogation regions or "patches" that each encompass a specific number of pixels of sufficiently different light intensity to enable them to be identified between the images [52]. Typically, patches are placed side by side or overlapping by half of the patch dimension to provide a detailed deformation field. In successive images, the patch displacements are tracked, so that the deformation field can be obtained.

The information needed to successfully identify a patch is generally provided in refractively matched media by tracers in the fluid. An alternative is to use selectively dyed or doped particles [20], suitable when the solid medium can retain the dye throughout the experiment. Finally, the granular texture itself, as a result of surface or embedded impurities, may be sufficient to distinguish particles as tracers.

The camera resolution, field of view and tracer seeding density dictate the minimum size of an image patch, and hence measurement resolution, that is suitable for analysis. As a general guide, a minimum of five tracers within a patch is considered sufficient to enable accurate identification of its location from image to image [44].

It should be noted that there are many "hybrid" PIV approaches [53, 54] available that allow for flow field measurements across scales, with variable light intensities and other demanding conditions. Open Source implementations of such PIV methods can also be found [55].

Particle Tracking Velocimetry involves determining the motion of individual particles, such as tracers, rather than groups of particles as used in PIV. Two advantages of PTV over PIV is (1) a reduced computational cost and, where low seeding density is desired. A low concentration of scatterers further helps to achieve deep optical access into a RI-matched medium. (2) PTV can achieve superior velocimetry results, especially regarding the measurement of fluctuations. Where this is not the case, PIV is often preferred due to its algorithmic robustness and flexibility.

4 Materials for LSM

Light sheet based imaging can be most easily done only in samples that are transparent in the range of wavelengths used. Transparency of a sample is set by two factors: absorbance and refraction of light passing through the sample. Both effects diminish the amount of light one has available for resolving flow fields after the light has passed through the medium. To optimize transparency, reducing adsorption and refraction are key. Many material designs to achieve said goals have been explored in the past, as covered by various past reviews [20, 21] and references therein. We refer the reader to these background works for further details. Here we aim to expand these references by introducing some lesser known materials from the literature while also introducing some new material designs not covered before.

4.1 Materials: simpler, safer, softer, biocompatible

The first option to make a transparent material is to find appropriate materials that index match. Finding a pair of solids and solvents that match in refractive index is challenging. However, the literature keeps revealing new index matched pairs that—to our knowledge—have not been reviewed before and are worthwhile candidates for realistic experiments. This section first approaches index matching from the perspective of the solid. Additionally, we will evoke the option of ionic liquids and deep eutectic solvents, which represent an under-studied opportunity to either decrease or increase the refractive index of a liquid.

Rigid particles — One candidate is the little used NH_4 I [57, 58]; another is the interesting choice of CaF_2 [59], which is a relatively low-toxicity, low-price material that can be used with water-glycerol mixtures as it does not dissolve in water. CaF_2 can be purchased as powder or crushed crystals; some professional optical components are made of this type of material. A drawback of CaF_2 and fluoride salts is that they are very dispersive at lower wavelengths.

Some other candidates have refractive indices that are close to that of water (~ 1.334), enabling imaging in environmentally relevant aqueous solutions. Note that many low refractive index materials usually have a fluorinated component in them; chemical synthesis of novel components with a low refractive index can use this strategy. One example is crushed Nafion, which is a polymer often used as a solid electrolyte in energy devices, that can keep bacteria and roots alive and allow for transparent soil options that allow for 3D imaging [60, 61]. Another promising candidate is the mineral cryolite (Na_3AlF_6) [62]. In both cases, crushed grains of Nafion or cryolite are rigid, with considerable heterogeneity in their shapes and sizes, similar to natural soils and sediments. Natural cryolite from mined deposits can be milled, sieved, and processed to mimic realistic soil textures. Surface hardness and impermeability make it compatible with interfacial chemistry assays including modifications via established methods such as silanization, amine, or carboxyl functionalization [63].

Deformable particles — Granular materials research can also be undertaken on soft particles, to study various properties of granular media not otherwise accessible, such as local stresses [64] or swelling dynamics [65]. Hydrogel beads can be synthesized in the lab [64] in various sizes [66] and can even be tuned in their frictional and optical (birefringent) response [64]. Another interesting method to study the internal dynamics of "soft granular" materials is to make index matched combinations of two immiscible fluids, or "chromatic emulsions" [67] which has even recently been accomplished in the soft matter workhorse poly(dimethylsiloxane) (PDMS) [68]. The canonical index matching components are the hydrogel beads sold by JRM Chemicals as "Snow". Other product names are GB7XX (via Educational Innovations) and Orbeez; various other online shops sell transparent and possibly colored version of these strongly swelling spheres, whose chemical composition is not always well specified, but is assumed to be polyacrylamide. Another option is to use Aquabeads / KI-GEL201 K-F2 [69] from Kuraray Chemical Co. Osaka, Japan.

One challenge is to make or find sub-millimeter hydrogel spheres (often known as "microgels"). One recent solution is to make agar-based hydrogel spheres [70]. We have found another potential solution for this challenge: Sephadex spheres. Sephadex spheres are micron-sized spheres made from crosslinked dextran, and widely used for decades in packed bed columns for gel chromatography. They come in various types, each with their own size distribution [71] and pore size features, all due to the ability of the dextran gels to separate large molecules by size by affecting their flow speed through the gels. Dextran contains pendant hydroxyl groups, providing convenient handles for covalent modification by, for instance, carbodiimide and carbodiimidazole coupling,[72] or by leveraging the hydroxyl's nucleophilicity towards isothiocyanates. Sephadex is widely available commercially. While it is not refractive index-matched with water, it can be index matched with water and PVP [73]; saturating the hydrogel with sucrose has also been shown to work [74]. Experiments with Sephadex packings have been used to model environmental processes, such as desiccation cracking of soils [75].

Another promising candidate is Carbopol, which is a dispersion of randomly crosslinked acrylic acid/alkyl acrylate copolymer microgels used as a rheological modifier in many commercial products. One route to creating defined granular packings is to disperse dry Carbopol granules (e.g., *Carbomer* 980 obtained from Ashland) into an aqueous medium of choice, where they swell into ~ 10 μm-diameter microgels. Because the microgels are highly swollen, they scatter very little light, rendering the medium optically transparent and suitable for direct 3D visualization via e.g., confocal laser-scanning fluorescence microscopy. The mesh size of the polymer network within each microgel is ~ 100 nm—too small to allow the passage of larger particulates, but large enough to allow for free diffusion of solvent and small solutes [76]. If the Carbopol is sufficiently concentrated, the swollen granules form a jammed packing; adjusting the Carbopol concentration provides a straightforward way to tune the packing fraction and, correspondingly, the sizes of the pores formed between the swollen grains [77–79]. Direct characterization of the pore space structure by tracking the long-time Brownian motion of fluorescent tracer particles reveals that, because of the heterogeneity in the Carbopol grain shapes and sizes, the

pore space is composed of randomly-oriented directed segments that resemble those observed in natural porous environments [79]. Ongoing work is exploring the synthesis of other classes of microgels of varying compositions, sizes, and shapes using techniques such as microfluidics, batch emulsions, or mechanical fragmentation [80].

Fluorescent soft particles — We have found that the Sephadex can be fluorescently labeled with a fairly easy one-step one-pot synthesis shown in Fig. 6a, adapted from literature [81]. Briefly, one disperses an amount of dry Sephadex beads as provided into DMSO and pyridine, adds fluorescein isothiocyanate (FITC) and then agitates the mixture at 95 °C for 2 h. We note that stirring with a magnetic stirring bar tends to break the Sephadex spheres. Purification can then be carried out by repeated washing of the Sephadex particles in ethanol to remove unreacted dye. Gentle centrifugation aids the recovery of particles. Ethanol is removed by evaporation, and the particles are dried and re-swollen in water. The procedure covalently links FITC to the hydroxyl groups of dextran. FRAP experiments show no recovery after bleaching, and thus confirm the covalent nature of the FITC-dextran bonds. Fig. 6b shows confocal imaging of the labeled Sephadex spheres.

Ionic liquids and deep eutectic solvents Index matching can be approached equally from the perspective of the liquid. Deep eutectic solvents (DES) are mixtures of solids that have a particularly deep melting point, often below room temperature [82]. Polarity and viscosity depend on the composition, and refractive indices have been tabulated for a large number of DES [83]. The addition of water to a polar DES reduces n_{D} and thus allows for precise matching. The use of DES as high-n_{D} for visualizing lung and intestinal tissue with light sheet microscopy is demonstrated in [84]. A mixture of imidazole and D-sorbitol provided the necessary transparency for a clearing agent, as well as the added benefit of solidifying the tissue without the addition of cross-linkers. Similar benefits could be realizable with ionic liquids, which also present a range of n_{D} and low melting points [85].

4.2 Material analysis: Christiansen filter

Refraction can be reduced by matching the index of the multiphase system as best as one can. A so-called "Christiansen filter" [12, 86] can aid in systematically tuning the indices of a two-phase system [87, 88]. Some practical but more limited variants have also been developed [89–91].

In a Christiansen filter [8, 88, 92, 93], a mixture of solid particles and liquids is exposed to light, and the transmitted light properties are examined as a function of a systematic variation of the liquid flowing through the filter and hence the particle packing. When the light used is polychromatic, dispersive effects can be visualized to find the liquid properties for which dispersion is minimal, and hence the filter is best index matched. One can also use a structured light source [21] or even text [20] to test for refractive index matching, although the latter is less quantitative. One of the interesting properties of Christiansen filters is that also particle size can be tuned [94], and they can be used with a wide variety of index matching substances, including borosilicate glass beads [95]. Even fibrous granular materials and textile fibers have been examined via these methods [96].

4.3 Using material artifacts

While unwelcome distortions can arise through refractive index mismatch, in some applications it may be used to advantage [97] found that thermal gradients in a transparent soil can be tracked through the gradual change in RI match between a fluid (which changes its RI with temperature) and solid (which does not, or much less so) [98]. also showed that the location of air-fluid interfaces (in this case, the air entry during shearing-induced dilation of a granular soil near the water table), and associated load-deformation behavior can be deduced in a refractively matched granular medium where there is an abrupt transition between transparent (fluid saturated) and opaque (air filled voids).

5 Applications of LSM

5.1 Peudostatic problems

The application of LSM in a refractively matched granular medium enables pseudostatic problems to be examined, such as the grain packing arrangement and gradual rearrangement. For example, a 2D plane may be illuminated by laser so that the solid particles appear dark compared to the fluid in which a fluorescent dye has been added. Continuous imaging of the material within a plane under the application of external load or destabilizing fluid flow then can enable particle rearrangement to be viewed within that plane. Contrast enhancement and deep learning to remove artifacts (e.g. streaks from laser mismatch) allows the particle edges to be distinguished. The thickness of the laser sheet is important here: the thinner the sheet, the more precise the definition of the edge of a particle. This is particularly important when non-spherical particles are used, where the location of particle edges is not easily predicted. Very thin laser sheets may best be achieved using open single fiber outputs with mirrors and lenses to direct and shape the light into a plane at the point of interest [99]. If a thicker laser sheet is acceptable or desired (e.g. for fluid tracer tracking), a patch-cable of multiple fibers can be directed to a Powell lens to produce

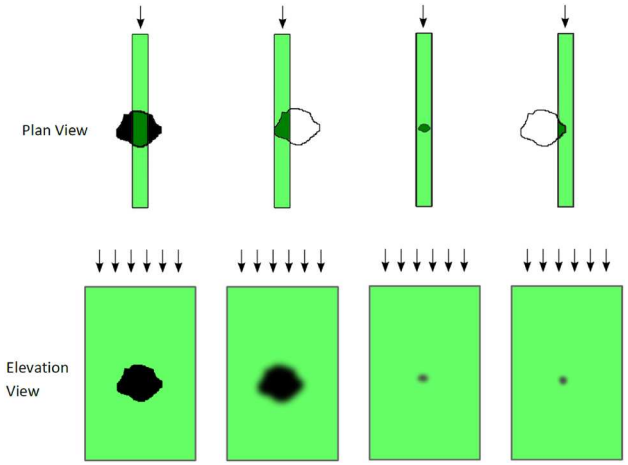

Fig. 5 Clarity of oblate rough particle identification according to light-sheet position and relative particle size. Image adapted from [56]

the light plane at its head. For uniform or near-uniform particle size distributions, such as monodisperse populations, it is straightforward to assess laser plane thickness requirements. For well-graded or highly polydisperse systems, the finest particle size will govern as illustrated in Fig. 5.

5.2 Deformation fluctuations

In a sheared or flowing granular system, the fluctuation in velocity of a particle around a mean trajectory suggests the presence of collisions. As a result, the measurement of fluctuation velocity is used to determine the collisional intensity of a flow [100–103]. The square or the fluctuation velocity may be termed the "granular temperature" whereupon the collisional agitation of granular material is considered analogous to a gas. The greater this agitation, the higher the granular temperature and the more collisional the flow. It turns out that the concepts of velocity fluctuations apply across a range of flow densities, from gas-like to very dense granular flows [104–106]. The concept of a granular temperature has therefore appeared in various theories on granular flows, including kinetic theory and kinetic elasto-plastic theories. How the microscopic fluctuations affect the macroscopic constitutive models is a major outstanding question in the field of granular flows [104, 106–109], hence measuring flow field fluctuations is an essential empirical capacity to develop. Most of these theoretical developments rely on numerical, discrete element method type simulations to provide the empirical lens on the microscopic fluctuations. To accurately *experimentally* measure velocity fluctuations in granular flows has proven challenging. Refractive index matching can be used to probe velocity fluctuations [110], albeit only in the dense, viscously damped flow regime. The immersion liquid usually provides overdamped dynamics for the particles in the suspension.

5.3 Applications to biological systems

Imaging transparent particulate media has immediate relevance for biological systems, as many organisms rely on the mechanical environment of soils for the growth, development and survival. Making laser-sheet compatible soils for biological systems comes with biocompatibility restrictions

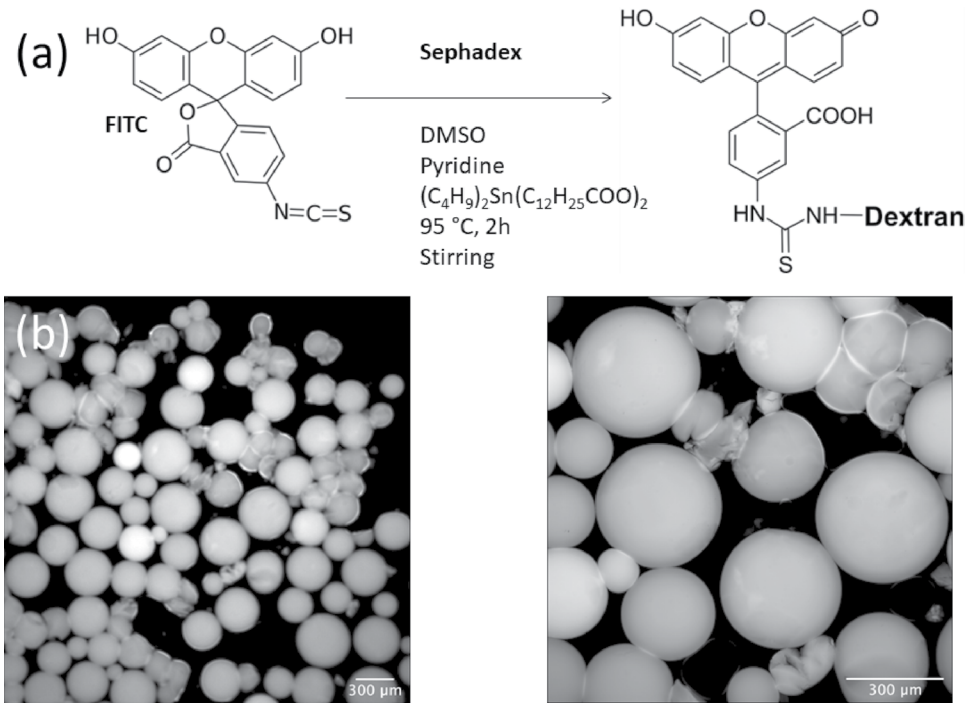

Fig. 6 **a** Synthesis of fluorescein-labeled Sephadex G75 by coupling of dextran pendant hydroxyl groups to fluorescein isothiocyanate (FITC). **b** Two confocal images of the labeled particles. Damage can be observed on some spheres

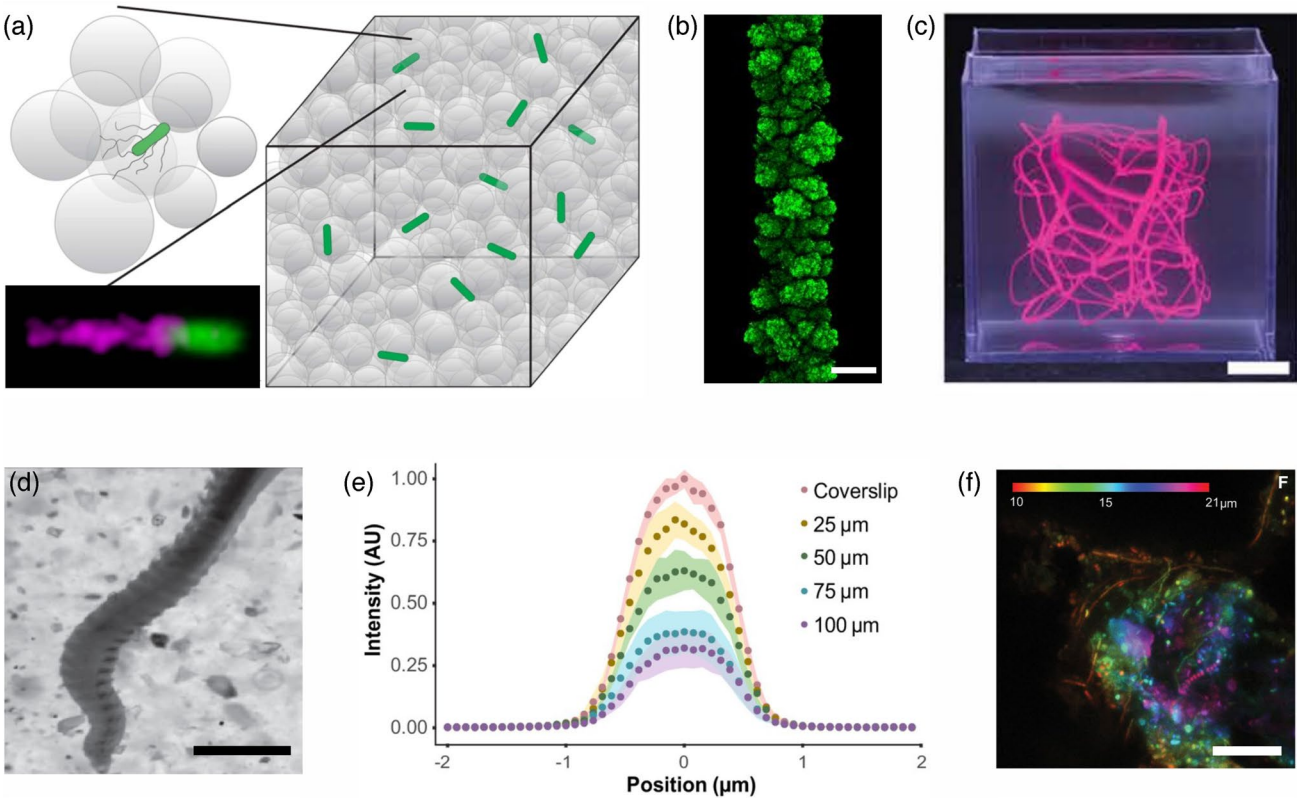

Fig. 7 Alternative methods to build transparent granular media: circumventing the index matching step using highly-swollen granular hydrogels **a**–**c** or cryolite **d**–**f**. **a** Schematic of 3D porous media, to study bacterial motility, made by jammed packings of Carbopol hydrogel particles. *E. coli* cells, shown in green (body) and magenta (flagella), are dispersed within the pores between the particles and imaged using confocal microscopy. The cell body length is about 2μm. Adapted from Bhattacharjee et al. [79]. **b** A colony of *E. coli*, 3D-printed in granular Carbopol media, displaying morphological instability and roughening after 24 h of colony growth in the absence of motility. Scale bar: 100μm. Adapted from Martinez-Calvo et al. [111]. **c** A vascular model printed into a granular microgel support bath. Scale bar: 1 cm. Adapted from Sexton et al. [112]. **d** Image of burrowing *Leioscoloplos pugettensis* worm in cryolite. Scale bar: 1 cm. Adapted from Francoeur et al [113]. **e** Fluorescence intensity profile of 1μm FITC beads embedded in cryolite matrix as a function of imaging depth. Adapted from Sharma et al [61]. **f** Sintered cryolite scaffold colonized by environmental microorganisms viewed via a maximum intensity projection of a confocal z-stack showing SYBR Gold-stained cells (green). The stack is color-coded to indicate the spatial distribution of cells throughout the depth of the scaffold ($10-21\mu m$). Scale bar: 10μm. Adapted from Quinn et al. [114]

on materials. Due to the biocompatibility of many hydrogel formulations, these systems have gained prominence as *in vitro* models to study biological processes in granular environments that mimic natural habitats, such as soil/sediments and biological tissues. Recent studies have used jammed packings of hydrogel grains to investigate microbial motility, encompassing a wide range of systems from single bacteria (Fig. 7a) [79], nematodes [115], and T-cells [116] to the collective chemotactic migration of bacterial populations [117]. These investigations have uncovered new biophysical insights into how cell behavior is shaped by confinement in a granular medium.

Because such jammed hydrogel grain packings are yield-stress materials, they can transition from solid-like to fluid-like states under applied stress. This property makes them attractive as matrices for embedded 3D printing, which enables the construction of macroscopic structures with microscale precision within such hydrogel packings [78]. As a result, they are increasingly finding use in biomedical science, such as to study biofilm growth in 3D environments (Fig. 7b) [111] and 3D-printing tissues and organoids (Fig. 7c) [112, 118–120].

Another alternative for studies of biological systems, particularly in granular media that model environmental soils/sediments, is cryolite. The first use of cryolite as a transparent granular medium dates back to pioneering studies in the 1970 s [121] which have continued in recent years for the visualization of burrowing organisms [113] (Fig. 7d). Recent advancements from Sharma et al. [61] have demonstrated the use of natural cryolite for high resolution fluorescence microscopy and single cell Raman spectroscopy in microcosms. Such transparent packings enable direct imaging of fluorescently labeled beads and cells in otherwise opaque soil-like environments (Fig. 7e). Yet, practical implementation is challenged by the presence of trace impurities such as siderite and internal defects that cause light scattering

and limit imaging depth. Synthetic cryolite powders, which are routinely produced and commercially available at scale, are amorphous and appear opaque in water. Recent work by Quinn et al. [114] introduces a sintering protocol under inert gas which crystallizes the synthetic cryolite to recover transparency. Sintered porous 'chips' of cryolite can be used for environmental ecology assays, including fluorescence in situ hybridization (FISH) to identify microorganisms from real environments (Fig. 7f). As new preparation techniques and advanced imaging protocols mature, the adoption of cryolite in biophysics, environmental microbiology, and granular media research is poised to expand significantly.

6 Conclusions

In this review, we have explored the diverse and evolving landscape of Light Sheet Microscopy (LSM) techniques for imaging granular materials. This optical approach to measuring deformation in materials has proven useful across a wide range of disciplines, including geophysics, geomechanics, chemical engineering, soft matter physics and biology. Focusing on imaging granular materials, we have highlighted the importance of selecting appropriate light sources, from broadband to single-wavelength options, and the role of some optical phenomena in generating contrast for imaging. We have reviewed the application of Christiansen filters and other systematic approaches to refractive index tuning can provide the field with more robust tools for optimizing imaging conditions.

We provide an outlook on the use and further development of advanced imaging techniques. We identify areas where LSM can immediately make a step forward in its range of application or in providing answers to open research questions. Summarizing, *(i)* wavefront shaping even from commercially available devices can further expand the capabilities of LSM, allowing for higher resolution, three-dimensional reconstructions of a wider range of granular systems, giving access to smaller particle sizes and different particle types. *(ii)* We highlight novel imaging solutions and the need for high-speed imaging of flow field structure and fluctuations to resolve some critical outstanding areas in the field of granular flow dynamics. *(iii)* We identify a range of materials to diversify the examples of materials that are amenable for 3D LSM imaging, including safer and simpler materials, but also softer and biocompatible materials for biophysics applications inside granular materials, such as root growth and animal burrowing.

By providing these priority areas embedded in historical and interdisciplinary references while including novel solutions, we aim to open new avenues for studying the mechanical behavior of an even wider variety of granular materials for an even wider range of engineering and scientific contexts.

Acknowledgements We thank Christopher Windows-Yule for stimulating us to write this perspective. We appreciate the discussion time provided to us at the Lorentz Center workshop "Image is everything" and at the third Salamina Grain Works workshop. We gratefully acknowledge sample testing by ZEISS Microscopy Customer Center Team (Oberkochen, Germany), specifically Dr. Steffen Burgold and Dr. Abel Pereira da Graça.

Author contributions JAD, SSD and EB wrote the main manuscript. JAD prepared Figs 1-4, the required LSM samples and associated text, EB prepared Fig 5 and associated text. ADF prepared Fig 6 and associated chemical synthesis and text. AAH, BVH and SSD prepared Fig 7 and associated text. All authors reviewed and approved publication of the manuscript.

Funding A.A.H. acknowledges funding support from the Center for the Physics of Biological Function at Princeton University.
S.S.D. acknowledges funding support from National Science Foundation (NSF) grant CBET-1941716 and the Camille Dreyfus Teacher-Scholar Program.

Data availability All relevant materials and methods are described in the main text. Raw figures from Zeiss microscopes and manuscript artwork are available upon reasonable request. No code was developed for this manuscript.

Declarations

Conflict of interest The authors declare no Conflict of interest.

Ethical approval Not applicable.

References

1. Truesdell, C., Noll, W.: The Non-linear Field Theories of Mechanics (Springer, 2004)
2. Morris, J.F.: Progress and challenges in suspension rheology. Rheol. Acta **62**, 617–629 (2023). https://doi.org/10.1007/s00397-023-01421-z
3. Jury, W. A., Horton, R.: Soil Physics (Wiley, 2004)
4. Barès, J., Cárdenas-Barrantes, M., Pinzón, G., Andò,E., Renouf, M., Viggiani, G., Azéma, E.:Compacting an assembly of soft balls far beyond the jammed state:iInsights from three-dimensional

imaging. Phys. Rev. E **108** (2023). https://doi.org/10.1103/physreve.108.044901
5. Abed Zadeh, A., Barés, J., Brzinski, T. A., Daniels, K. E., Dijksman, J., Docquier, N., Everitt, H. O., Kollmer, J. E., Lantsoght, O., Wang, D., Workamp, M., Zhao, Y., Zheng, H.: Enlightening force chains: a review of photoelasticimetry in granular matter. Granul. Matter **21** (2019). https://doi.org/10.1007/s10035-019-0942-2
6. Joseph Antony, S.: Power of photo-stress analysis in unravelling the mechanics of granular materials and its applications in interdisciplinary research. Opt. Lasers Eng. **183**, 108512 (2024). https://doi.org/10.1016/j.optlaseng.2024.108512
7. Li, W., Juanes, R.: Dynamic imaging of force chains in 3D granular media. Proc. Natl. Acad. Sci. **121** (2024). https://doi.org/10.1073/pnas.2319160121
8. McAlister, E. D.:The Christiansen light filter: its advantages and limitations. Smithsonian Miscellaneous Collections (1935)
9. d'Ambrosio, E., Blanc, F., Lemaire, E.: Velocity distributions, dispersion and stretching in three-dimensional porous media. J. Fluid Mech. **967**, A34 (2023)
10. Siedentopf, H., Zsigmondy, R.: Über Sichtbarmachung und Groessenbestimmung ultramikroskopischer Teilchen, mit besonderer Anwendung auf Goldrubinglaesern. Ann. Phys. **10**, 1 (1903)
11. Konagai, K., Tamura, C., Rangelow, P., Matsushima, T.: Laser-aided tomography: a tool for visualization of changes in the fabric of granular assemblage. Doboku Gakkai Ronbunshu **1992**, 25 (1992)
12. Christiansen, C.: Untersuchungen über die optischen Eigenschaften von fein vertheilten Körpern. Ann. Phys. **259**, 298 (1884)
13. Girkin, J.M., Carvalho, M.T.: The light-sheet microscopy revolution. J. Opt. **20**, 053002 (2018)
14. Dodt, H.-U., Leischner, U., Schierloh, A., Jährling, N., Mauch, C.P., Deininger, K., Deussing, J.M., Eder, M., Zieglgänsberger, W., Becker, K.: Ultramicroscopy: three-dimensional visualization of neuronal networks in the whole mouse brain. Nat. Methods **4**, 331 (2007)
15. Voie, A.H., Burns, D., Spelman, F.: Orthogonal-plane fluorescence optical sectioning: Three-dimensional imaging of macroscopic biological specimens. J. Microsc. **170**, 229 (1993)
16. Huisken, J., Stainier, D.Y.: Selective plane illumination microscopy techniques in developmental biology. Development **136**, 1963 (2009)
17. Walker, D.A.: A fluorescence technique for measurement of concentration in mixing liquids. Sci. Instrum. J. Phys. E **20**, 217–224 (1987). https://doi.org/10.1088/0022-3735/20/2/019
18. Hanson, R.K.: Planar laser-induced fluorescence imaging. J. Quant. Spectrosc. Radiat. Transf. **40**, 343–362 (1988). https://doi.org/10.1016/0022-4073(88)90125-2
19. Crimaldi, J.P.: Planar laser induced fluorescence in aqueous flows. Exp. Fluids **44**, 851–863 (2008). https://doi.org/10.1007/s00348-008-0496-2
20. Wiederseiner, S., Andreini, N., Epely-Chauvin, G., Ancey, C.: Refractive-index and density matching in concentrated particle suspensions: a review. Exp. Fluids **50**, 1183 (2011). (**publisher: Springer**)
21. Dijksman,J. A., Rietz, F., Lőrincz, K. A., Van Hecke, M., Losert, W.: Invited Article: Refractive index matched scanning of dense granular materials Christiansen-type transparent porous media for flow studies. Rev. Sci. Instrum. **83** (2012) https://doi.org/10.1063/1.3674173
22. Andò, E., Viggiani, G., Hall, S.A., Desrues, J.: Experimental micro-mechanics of granular media studied by x-ray tomography: recent results and challenges. Géotech. Lett. **3**, 142–146 (2013). https://doi.org/10.1680/geolett.13.00036
23. Besseling, R., Damen, M., Wijgergangs, J., Hermes, M., Wynia, G., Gerich, A.: New unique PAT method and instrument for real-time inline size characterization of concentrated, flowing nanosuspensions. Eur. J. Pharm. Sci. **133**, 205 (2019)
24. Spicer, P.T., Hosseini, M., Babayekhorasani, F.: Complex fluid product microstructure imaging with light sheet fluorescence microscopy. Curr. Op. Coll. Interf. Sci. **77**, 101916 (2025). https://doi.org/10.1016/j.cocis.2025.101916
25. Masters,B. R.: Superresolution Optical Microscopy: The Quest for Enhanced Resolution and Contrast, Springer (2020) https://link.springer.com/book/10.1007/978-3-030-21691-7
26. Buchmann, N.A., Willert, C.E., Soria, J.: Pulsed, high-power LED illumination for tomographic particle image velocimetry. Exp. Fluids **53**, 1545 (2012)
27. Willert, C., Stasicki, B., Klinner, J., Moessner, S.: Pulsed operation of high-power light emitting diodes for imaging flow velocimetry. Meas. Sci. Technol. **21**, 075402 (2010). https://doi.org/10.1088/0957-0233/21/7/075402
28. Harshani, H., Galindo-Torres, S., Scheuermann, A., Muhlhaus, H.: Experimental study of porous media flow using hydro-gel beads and LED based PIV. Meas. Sci. Technol. **28**, 015902 (2017)
29. Power, R.M., Huisken, J.: A guide to light-sheet fluorescence microscopy for multiscale imaging. Nat. Methods **14**, 360–373 (2017). https://doi.org/10.1038/nmeth.4224
30. Thorlabs—thorlabs.com, [Accessed 23-12-2025] https://www.thorlabs.com/compact-laser-modules-with-usb-connector?tabName=Overview
31. Chen, B.-C., Legant, W.R., Wang, K., Shao, L., Milkie, D.E., Davidson, M.W., Janetopoulos, C., Wu, X.S., Hammer, J.A., III., Liu, Z., et al.: Lattice light-sheet microscopy: imaging molecules to embryos at high spatiotemporal resolution. Science **346**, 1257998 (2014)
32. Yu, H., Park, J., Lee, K., Yoon, J., Kim, K., Lee, S., Park, Y.: Recent advances in wavefront shaping techniques for biomedical applications. Curr. Appl. Phys. **15**, 632 (2015)
33. Koukourakis, N., Fregin, B., König, J., Büttner, L., Czarske, J.W.: Wavefront shaping for imaging-based flow velocity measurements through distortions using a Fresnel guide star. Opt. Express **24**, 22074 (2016)
34. Hassan, Y.A., Dominguez-Ontiveros, E.: Flow visualization in a pebble bed reactor experiment using PIV and refractive index matching techniques. Nucl. Eng. Des. **238**, 3080 (2008)
35. Ni, Q., Hird, C.C., Guymer, I.: Physical modelling of pile penetration in clay using transparent soil and particle image velocimetry. Geótechnique **60**, 121 (2010)
36. Sang, Y., Zhao, J., Duan, F., Sun, W., Zhao, H.: A novel automatic device to measure deformation inside transparent soil based on digital image correlation technology. Meas. Sci. Technol. **30**, 035202 (2019)
37. Erpelding, M., Amon, A., Crassous, J.: Diffusive wave spectroscopy applied to the spatially resolved deformation of a solid. Phys. Rev. E **78**. https://doi.org/10.1103/physreve.78.046104, (2008)
38. Zakharov, P., Völker, A., Wyss, M., Haiss, F., Calcinaghi, N., Zunzunegui, C., Buck, A., Scheffold, F., Weber, B.: Dynamic laser speckle imaging of cerebral blood flow. Dynamic laser speckle imaging of cerebral blood flowDynamic laser speckle imaging of cerebral blood flow. Opt. Express **17**(13904),(2009). https://doi.org/10.1364/oe.17.013904
39. Stöhr, M., Roth, K., Jähne, B.: Measurement of 3D pore-scale flow in index-matched porous media. Exp. Fluids **35**, 159 (2003)
40. Gualda, E.J., Vale, T., Almada, P., Feijó, J.A., Martins, G.G., Moreno, N.: OpenSpinMicroscopy: an open-source integrated microscopy platform. Nat. Methods **10**, 599 (2013)
41. Willert, C. E., Klinner, J.: Event-based imaging velocimetry: an assessment of event-based cameras for the measurement of fluid

flows. Exp. Fluids **63**, (2022). https://doi.org/10.1007/s00348-022-03441-6
42. Nakamura, R., Domae, M., Morimoto, T., Izumikawa, T., Fujii, H.: Dynamic visualization of construction sites with machine-borne sensors toward automated earth moving. J. Robot. Mechatron. **36**, 294–308 (2024). https://doi.org/10.20965/jrm.2024.p0294
43. Willert, C. E., Klinner, J.: Dynamic wall shear stress measurement using event-based 3d particle tracking. Exp. Fluids **66**, (2025). https://doi.org/10.1007/s00348-024-03946-2
44. Sanvitale, N., Zhao, B., Bowman, E., O'Sullivan, C.: Particle-scale observation of seepage flow in granular soils using PIV and CFD. Géotechnique **73**, 71 (2023)
45. Heyman, J.: A fast multi-object tracking algorithm for motion estimation. Comput. Geosci. **128**, 11 (2019). https://doi.org/10.1016/j.cageo.2019.03.007
46. Moroni, M., Cushman, J.H.: Statistical mechanics with three-dimensional particle tracking velocimetry experiments in the study of anomalous dispersion. II. Exp. Phys. Fluids **13**, 81 (2001). https://doi.org/10.1063/1.1328076
47. Wan, Y., McDole, K., Keller, P.J.: Light-sheet microscopy and its potential for understanding developmental processes. Annu. Rev. Cell Dev. Biol. **35**, 655 (2019)
48. Elisa, Z., Toon, B., De Smedt, S.C., Katrien, R., Kristiaan, N., Kevin, B.: Technical implementations of light sheet microscopy. Microsc. Res. Tech. **81**, 941 (2018)
49. Von Wangenheim, D., Hauschild, R., Friml, J.: Light sheet fluorescence microscopy of plant roots growing on the surface of a gel: a simple chamber for long-term confocal imaging of root and hypocotyl development. J. Vis. Exp. **123**, 55044 (2017)
50. Dondeti, S., Miao, C., Tippur, H.: A note on measuring mechanical fields in 3-D solids using digital gradient sensing and refractive index matching. Exp. Mech. **63**, 263 (2023)
51. Thielicke, W., Stamhuis, E. J.: PIVlab–towards user-friendly, affordable and accurate digital particle image velocimetry in MATLAB. J. Open Res. Softw. (2014). https://doi.org/10.5334/jors.bl
52. White, D., Take, W., Bolton, M.: Soil deformation measurement using particle image velocimetry (PIV) and photogrammetry. Géotechnique **53**, 619 (2003)
53. Becker, F., Wieneke, B., Petra, S., Schroder, A., Schnorr, C.: Variational adaptive correlation method for flow estimation. IEEE Trans. Image Process. **21**, 3053–3065 (2012). https://doi.org/10.1109/tip.2011.2181524
54. Yamamoto, F., Ishikawa, M.: A review of the recent PIV studies–from the basics to the hybridization with CFD. J. Flow Control Meas. Vis. **10**, 117–147 (2022). https://doi.org/10.4236/jfcmv.2022.104008
55. Liu, T.: OpenOpticalFlow: an open source program for extraction of velocity fields from flow visualization images. J. Open Res. Softw. **5**, 29 (2017). https://doi.org/10.5334/jors.168
56. Hunter, R. P.: Development of transparent soil testing using planar laser induced fluorescence in the study of internal erosion of filters in embankment dams. Development of transparent soil testing using planar laser induced fluorescence in the study of internal erosion of filters in embankment dams, Ph.D. thesis, University of Canterbury. Geological Sciences (2012)
57. de Jong, G. d. J. : Longitudinal and transverse diffusion in granular deposits. Soil Mech. Transp. Porous Med. Selected works of G. De Josselin de Jong, 261 (2006) https://doi.org/10.1029/TR039i001p00067
58. Lamelas, F.: Index of refraction, density, and solubility of ammonium iodide solutions at high pressure. J. Phys. Chem. B **117**, 2789 (2013)
59. Heller, J.P.: Christiansen-type transparent porous media for flow studies. Rev. Sci. Instrum. **30**, 1056 (1959)
60. Downie, H., Holden, N., Otten, W., Spiers, A. J., Valentine, T. A., Dupuy, L. X.: Transparent soil for imaging the rhizosphere. PLOS One 44276 (2012)
61. Sharma, K., Palatinszky, M., Nikolov, G., Berry, D., Shank, E.A.: Transparent soil microcosms for live-cell imaging and non-destructive stable isotope probing of soil microorganisms. Elife **9**, 56275 (2020)
62. Pauly, H.: Cryolite, chiolite and cryolithonite: optical data redetermined. Bull. Geol. Soc. Den. **26**, 95 (1977)
63. Sypabekova, M., Hagemann, A., Rho, D., Kim, S.: 3-Aminopropyltriethoxysilane (APTES) deposition methods on oxide surfaces in solution and vapor phases for biosensing applicati.3-Aminopropyltriethoxysilane (APTES) deposition methods on oxide surfaces in solution and vapor phases for biosensing applications. Biosensors **13**, 36 (2022)
64. Workamp, M., Dijksman, J.A.: Contact tribology also affects the slow flow behavior of granular emulsions. J. Rheol. **63**, 275 (2019)
65. Louf, J.-F., Lu, N.B., O'Connell, M.G., Cho, H.J., Datta, S.S.: Under pressure: hydrogel swelling in a granular medium. Sci. Adv. **7**, 2711 (2021)
66. Workamp, M., Alaie, S., Dijksman, J. A.: Coaxial air flow device for the production of millimeter-sized spherical hydrogel particles. Rev. Sci. Instrum. **87** (2016)
67. Holmes, H.N., Cameron, D.H.: Chromatic emulsions. J. Am. Chem. Soc. **44**, 71 (1922)
68. Duraivel, S., Laurent, D., Rajon, D.A., Scheutz, G.M., Shetty, A.M., Sumerlin, B.S., Banks, S.A., Bova, F.J., Angelini, T.E.: A silicone-based support material eliminates interfacial instabilities in 3D silicone printing. Science **379**, 1248–1252 (2023). https://doi.org/10.1126/science.ade4441
69. Lo, H.-C., Tabe, K., Iskander, M., Yoon, S.-H.: A transparent water-based polymer for simulating multiphase flow. Geotech. Test. J. **33**, 1 (2010)
70. Sreepadmanabh, M., Ganesh, M., Bhat, R., Bhattacharjee, T.: Jammed microgel growth medium prepared by flash-solidification of agarose for 3D cell culture and 3D bioprinting. Biomed. Mater. **18**, 045011 (2023). https://doi.org/10.1088/1748-605x/acd315
71. De Mets, M., Lagasse, A.: Gel chromatography column packings as observed with the scanning electron microscope. J. Chromatogr. A **47**, 487 (1970)
72. Bamford, C.H., Middleton, L.P., Ai-Lamee, K.G.: Studies of the esterification of dextran: routes to bioactive polymers and graft copolymers. Polymer **27**, 1981 (1986)
73. Dijksman, J. A., Brodu, N., Behringer, R. P.: Refractive index matched scanning and detection of soft particles. Rev. Sci. Instrum. **88** (2017)
74. Franklin, J., Wang, Z.Y.: Refractive index matching: a general method for enhancing the optical clarity of a hydrogel matrix. Chem. Mater. **14**, 4487 (2002)
75. Cho, H.J., Datta, S.S.: Scaling law for cracking in shrinkable granular packings. Phys. Rev. Lett. **123**, 158004 (2019)
76. Bhattacharjee, T., Kabb, C.P., O'Bryan, C.S., Urueña, J.M., Sumerlin, B.S., Sawyer, W.G., Angelini, T.E.: Polyelectrolyte scaling laws for microgel yielding near jamming. Soft Matter **14**, 1559 (2018)
77. Bhattacharjee, T., Gil, C.J., Marshall, S.L., Urueña, J.M., O'Bryan, C.S., Carstens, M., Keselowsky, B., Palmer, G.D., Ghivizzani, S., Gibbs, C.P., et al.: Liquid-like solids support cells in 3D. ACS Biomater. Sci. Eng. **2**, 1787 (2016)
78. Bhattacharjee, T., Zehnder, S.M., Rowe, K.G., Jain, S., Nixon, R.M., Sawyer, W.G., Angelini, T.E.: Writing in the granular gel medium. Sci. Adv. **1**, e1500655 (2015)
79. Bhattacharjee, T., Datta, S.S.: Bacterial hopping and trapping in porous media. Nat. Commun. **10**, 2075 (2019)

80. Muir, V.G., Qazi, T.H., Shan, J., Groll, J., Burdick, J.A.: Influence of microgel fabrication technique on granular hydrogel properties. ACS Biomater. Sci. Eng. **7**, 4269 (2021)
81. Anwar, M., Nadeem, F., Faiz, S.: A review of synthesis of fluorescein based advanced materials. Int. J. Chem. Biochem. Sci. **14**, 120 (2018). www.iscientific.org/Journal.html
82. Hansen, B.B., Spittle, S., Chen, B., Poe, D., Zhang, Y., Klein, J.M., Horton, A., Adhikari, L., Zelovich, T., Doherty, B.W., Gurkan, B., Maginn, E.J., Ragauskas, A., Dadmun, M., Zawodzinski, T.A., Baker, G.A., Tuckerman, M.E., Savinell, R.F., Sangoro, J.R.: Deep Eutectic solvents: a review of fundamentals and applications. Chem. Rev. **121**, 1232 (2021). https://doi.org/10.1021/acs.chemrev.0c00385
83. Luan, J., Cheng, Y., Xue, F., Cui, L., Wang, D.: Refractive index of 48 neat deep eutectic solvents and of selected mixtures: effect of temperature, hydrogen-bonding donors, hydrogen-bonding acceptors, mole ratio, and water. ACS Omega **8**, 25582 (2023). https://doi.org/10.1021/acsomega.3c03502
84. Qin, R., Huang, P., Zhao, Q., Rao, Y., Qiu, Q. Quan, W., Ye, H., liao, J., Fang, F., Ma, H., Wu, K.: Supramolecular self-assembling hydrogel based on imidazole/D-sorbitol deep eutectic solvent for tissue clearance. J. Mol. Liquids **409** (2024). https://doi.org/10.1016/j.molliq.2024.125382
85. Pachernegg, L., Maier, J., Yagmur, R., Damm, M., Kalb, R., Coclite, A.M., Spirk, S.: Physicochemical properties of 20 ionic liquids prepared by the carbonate-based IL (CBILS) process. J. Chem. Eng. Data **69**, 1814 (2024). https://doi.org/10.1021/acs.jced.3c00687
86. Christiansen, C.: Untersuchungen über die optischen Eigenschaften von fein vertheilten Körpern. Ann. Phys. **260**, 439 (1885)
87. Buerger, M.: Generalized microscopy and the two-wave-length microscope. J. Appl. Phys. **21**, 909 (1950)
88. Raman, C., Viswanathan, K.: A generalised theory of the Christiansen experiment. In: Proceedings of the Indian Academy of Sciences-Section A, vol. 41, pp. 55–60. Springer (1955)
89. Eveleth, W. T.: Measurement of Particle Size and Distribution in a Suspension. Measurement of Particle Size and Distribution in a Suspension, Ph.D. thesis, Union College (1927)
90. Pickels, E.G.: Sedimentation in the angle centrifuge. J. Gen. Physiol. **26**, 341 (1943)
91. Goldsmith, H., Mason, S.: The microrheology of suspensions. The microrheology of suspensions., Ph.D. thesis, McGill University (1961)
92. Anderson, J.S.: Immersion refractometry. Trans. Opt. Soc. **21**, 195 (1920)
93. Raman, C.: The theory of the Christiansen experiment. In Proceedings of the Indian Academy of Sciences-Section A, vol. 29, pp. 381–390. Springer (1949)
94. Denmark, H., Cady, W.M.: Optimum grain size in the Christiansen filter. JOSA **25**, 330 (1935)
95. Deutsch, E.: Optical scanning of liquid concentration in flow studies with porous models. Nature **185**, 675 (1960)
96. Fox, K.R.: Refractive indices of textile fibres: double variation method for the determination of. Text. Res. **10**, 79 (1939)
97. Siemens, G., Mumford, K., Kucharczuk, D.: Characterization of transparent soil for use in heat transport experiments. Geotech. Test. J. **38**, 620 (2015)
98. Parera Morales, F., Siemens, G., McKellar, M., Pinyol, N., Alonso, E., Take, W.: Footprints on the beach: visualising dilation-induced air entry. Géotechnique (2024)
99. Souzy, M., Lhuissier, H., Méheust, Y., Le Borgne, T., Metzger, B.: Velocity distributions, dispersion and stretching in three-dimensional porous media. J. Fluid Mech. **891**, A16 (2020)
100. Jenkins, J., Savage, S.: A theory for the rapid flow of identical, smooth, nearly elastic, spherical particles. J. Fluid Mech. **130**, 187 (1983)
101. Walton, O.R., Braun, L.: Viscosity, granular?temperature, and stress calculations for shearing assemblies of inelastic, frictional disks. J. Rheol. **30**, 949–980 (1986). https://doi.org/10.1122/1.549893
102. Cody, G., Goldfarb, D., Storch, G., Jr., Norris, A.: Particle granular temperature in gas fluidized beds. Powder Technol. **87**, 211 (1996)
103. Losert, W., Cooper, D., Delour, J., Kudrolli, A., Gollub, J.P.: Velocity statistics in excited granular media. Chaos Interdiscip. J. Nonlinear Sci. **9**, 682 (1999)
104. Goldhirsch, I.: Introduction to granular temperature. Powder Technol. **182**, 130–136 (2008). https://doi.org/10.1016/j.powtec.2007.12.002
105. Zhang, Q., Kamrin, K.: Microscopic description of the granular fluidity field in nonlocal flow modeling. Phys. Rev. Lett. **118**, 058001 (2017)
106. Berzi, D.: On granular flows: from kinetic theory to inertial rheology and nonlocal constitutive models. Phys. Rev. Fluids **9**, 034304 (2024)
107. Berzi, D., Jenkins, J. T.: Fluidity, anisotropy, and velocity correlations in frictionless, collisional grain flows. Phys. Rev. Fluids **3**. https://doi.org/10.1103/physrevfluids.3.094303 (2018)
108. Kim, S., Kamrin, K.: Power-law scaling in granular rheology across flow geometries. Phys. Rev. Lett. **125** (2020). https://doi.org/10.1103/physrevlett.125.088002
109. Kamrin, K., Hill, K.M., Goldman, D.I., Andrade, J.E.: Advances in modeling dense granular media. Annu. Rev. Fluid Mech. **56**, 215–240 (2024). https://doi.org/10.1146/annurev-fluid-121021-022045
110. Wandersman, E., Dijksman, J.A., Van Hecke, M.: Particle diffusion in slow granular bulk flows. Europhys. Lett. **100**, 38006 (2012)
111. Martínez-Calvo, A., Bhattacharjee, T., Bay, R.K., Luu, H.N., Hancock, A.M., Wingreen, N.S., Datta, S.S.: Morphological instability and roughening of growing 3D bacterial colonies. Proc. Natl. Acad. Sci. **119**, e2208019119 (2022)
112. Sexton, Z.A., Rütsche, D., Herrmann, J.E., Hudson, A.R., Sinha, S., Du, J., Shiwarski, D.J., Masaltseva, A., Solberg, F.S., Pham, J., et al.: Rapid model-guided design of organ-scale synthetic vasculature for biomanufacturing. Science **388**, 1198 (2025)
113. Francoeur, A.A., Dorgan, K.M.: Burrowing behavior in mud and sand of morphologically divergent polychaete species (Annelida: Orbiniidae). Biol. Bull. **226**, 131 (2014)
114. Quinn, L.K., Sharma, K., Faber, K.T., Orphan, V.J.: Clear as mud redefined: Tunable transparent mineral scaffolds for visualizing microbial processes below ground. PNAS Nexus **4**, 118 (2025)
115. Dey, S., Sreepadmanabh, M., Kundu, S., Arun, A. B., Koushika, S. P., Thutupalli, S., Hewitt, D., Bhattacharjee, T.: Physical confinement regulates transition in nematode motility. bioRxiv 2025 (2025)
116. Morley, C.D., Flores, C.T., Drake, J.A., Moore, G.L., Mitchell, D.A., Angelini, T.E.: Spatiotemporal T cell dynamics in a 3D bioprinted immunotherapy model. Bioprinting **28**, 00231 (2022)
117. Bhattacharjee, T., Amchin, D.B., Ott, J.A., Kratz, F., Datta, S.S.: Chemotactic migration of bacteria in porous media. Biophys. J . **120**, 3483 (2021)
118. Daly, A.C., Riley, L., Segura, T., Burdick, J.A.: Hydrogel microparticles for biomedical applications. Nat. Rev. Mater. **5**, 20 (2020)
119. Riley, L., Schirmer, L., Segura, T.: Granular hydrogels: emergent properties of jammed hydrogel microparticles and their applications in tissue repair and regeneration. Curr. Opin. Biotechnol. **60**, 1 (2019)

120. Hinton, T.J., Jallerat, Q., Palchesko, R.N., Park, J.H., Grodzicki, M.S., Shue, H.-J., Ramadan, M.H., Hudson, A.R., Feinberg, A.W.: Three-dimensional printing of complex biological structures by freeform reversible embedding of suspended hydrogels. Sci. Adv. **1**, e1500758 (2015)
121. Josephson, R.K., Flessa, K.W.: Cryolite: a medium for the study of burrowing aquatic organisms 1. Limnol. Oceanogr. **17**, 134 (1972)